NASA/CR—2003-212582

Laser Synthesis of Supported Catalysts for Carbon Nanotubes

Randall L. Vander Wal
National Center for Microgravity Research, Cleveland, Ohio

Thomas M. Ticich and Leif J. Sherry
Centenary College of Louisiana, Shreveport, Louisiana

Lee J. Hall
National Center for Microgravity Research, Cleveland, Ohio

September 2003

The NASA STI Program Office . . . in Profile

Since its founding, NASA has been dedicated to the advancement of aeronautics and space science. The NASA Scientific and Technical Information (STI) Program Office plays a key part in helping NASA maintain this important role.

The NASA STI Program Office is operated by Langley Research Center, the Lead Center for NASA's scientific and technical information. The NASA STI Program Office provides access to the NASA STI Database, the largest collection of aeronautical and space science STI in the world. The Program Office is also NASA's institutional mechanism for disseminating the results of its research and development activities. These results are published by NASA in the NASA STI Report Series, which includes the following report types:

- TECHNICAL PUBLICATION. Reports of completed research or a major significant phase of research that present the results of NASA programs and include extensive data or theoretical analysis. Includes compilations of significant scientific and technical data and information deemed to be of continuing reference value. NASA's counterpart of peer-reviewed formal professional papers but has less stringent limitations on manuscript length and extent of graphic presentations.

- TECHNICAL MEMORANDUM. Scientific and technical findings that are preliminary or of specialized interest, e.g., quick release reports, working papers, and bibliographies that contain minimal annotation. Does not contain extensive analysis.

- CONTRACTOR REPORT. Scientific and technical findings by NASA-sponsored contractors and grantees.

- CONFERENCE PUBLICATION. Collected papers from scientific and technical conferences, symposia, seminars, or other meetings sponsored or cosponsored by NASA.

- SPECIAL PUBLICATION. Scientific, technical, or historical information from NASA programs, projects, and missions, often concerned with subjects having substantial public interest.

- TECHNICAL TRANSLATION. English-language translations of foreign scientific and technical material pertinent to NASA's mission.

Specialized services that complement the STI Program Office's diverse offerings include creating custom thesauri, building customized databases, organizing and publishing research results . . . even providing videos.

For more information about the NASA STI Program Office, see the following:

- Access the NASA STI Program Home Page at ***http://www.sti.nasa.gov***

- E-mail your question via the Internet to help@sti.nasa.gov

- Fax your question to the NASA Access Help Desk at 301–621–0134

- Telephone the NASA Access Help Desk at 301–621–0390

- Write to:
  NASA Access Help Desk
  NASA Center for AeroSpace Information
  7121 Standard Drive
  Hanover, MD 21076

NASA/CR—2003-212582

Laser Synthesis of Supported Catalysts for Carbon Nanotubes

Randall L. Vander Wal
National Center for Microgravity Research, Cleveland, Ohio

Thomas M. Ticich and Leif J. Sherry
Centenary College of Louisiana, Shreveport, Louisiana

Lee J. Hall
National Center for Microgravity Research, Cleveland, Ohio

Prepared under Cooperative Agreement NCC3–975

National Aeronautics and
Space Administration

Glenn Research Center

September 2003

Acknowledgments

This work was supported under the Revolutionary Aerospace Concepts Project (RAC), part of the Research and Technology Base Propulsion and Power Program and by a NASA Glenn Strategic Research Fund (SRF) award, both administered through NASA cooperative agreement NAC3–544 with the National Center for Microgravity Research on Fluids and Combustion (NCMR) at the NASA Glenn Research Center. Mr. Thomas Ticich and Mr. Leif Sherry acknowledge support through the Ohio Aerospace Institute Collaborative Aerospace program for visiting summer faculty and accompanying students. The authors gratefully acknowledge David R. Hull for the HRTEM imaging.

This report contains preliminary findings, subject to revision as analysis proceeds.

Available from

NASA Center for Aerospace Information
7121 Standard Drive
Hanover, MD 21076

National Technical Information Service
5285 Port Royal Road
Springfield, VA 22100

Available electronically at http://gltrs.grc.nasa.gov

Laser Synthesis of Supported Catalysts for Carbon Nanotubes

Randall L. Vander Wal*
National Center for Microgravity Research
Cleveland, Ohio 44135

Thomas M. Ticich and Leif J. Sherry
Centenary College of Louisiana
Shreveport, Louisiana 71134

Lee J. Hall
National Center for Microgravity Research
Cleveland, Ohio 44135

Abstract

Four methods of laser assisted catalyst generation for carbon nanotube (CNT) synthesis have been tested. These include pulsed laser transfer (PLT), photolytic deposition (PLD), photothermal deposition (PTD) and laser ablation deposition (LABD). Results from each method are compared based on CNT yield, morphology and structure. Under the conditions tested, the PLT was the easiest method to implement, required the least time and also yielded the best patternation. The photolytic and photothermal methods required organometallics, extended processing time and partial vacuums. The latter two requirements also held for the ablation deposition approach. In addition to control of the substrate position, controlled deposition duration was necessary to achieve an active catalyst layer. Although all methods were tested on both metal and quartz substrates, only the quartz substrates proved to be inactive towards the deposited catalyst particles.

Introduction

A vast array of methods for thin film synthesis has been explored for numerous applications. In particular, the methods of pulsed laser transfer (PLT), photolytic deposition (PLD), photothermal deposition (PTD) and laser ablation deposition (LABD) have been tested and applied to thin film formation or patterned deposition (refs. 1 to 4). Common to each of these methods is the inception of the thin film, which begins at the atomic/molecular level and ultimately grows to macroscopic dimensions (ref. 5). Fundamental studies have shown that as a submonolayer, the "film" consists of islands, discrete particles or clusters that depend both upon the substrate temperature and mobility of the atoms upon the substrate material (refs. 6 and 7). In this work we sought to exploit this initial structure, using short deposition times in order to create submonolayers of catalytically active metals.

A discontinuous thin film comprised of small clusters and larger islands is potentially well suited towards catalysis of CNT's. CNT formation begins only at those sites where grain boundaries, edge sites or lattice dislocations allow carbon solvation and dissolution for multiwalled carbon nanotube (MWNT) or nanofiber growth via either a tip or base growth mechanism (ref. 8). Their synthesis typically requires catalyst particles within the size range of a few nanometers. Current methods for achieving such sizes

* Corresponding author: 21000 Brookpark Road, Cleveland, Ohio 44135. Phone: 216–433–9065, Fax: 216–433–3793, E-mail: Randy.VanderWal@grc.nasa.gov

uniformly dispersed upon a solid, rigid support material employ sophisticated electronic patterning processes such as sputtering, electron beam evaporation, and/or lithography (ref. 9). These techniques require high voltages or currents, an expensive apparatus and high vacuum and ultraclean conditions. Alternatives such as wet chemical techniques can introduce contaminants and do not yet offer the level of control characteristic of the aforementioned techniques. In contrast, optical methods offer many advantages over these techniques in creating metal patterns with high spatial resolution. Moreover, a wide range of parameters is available such as irradiation time, laser fluence, the nature of the ambient environment, the phase of the reactant and its vapor pressure.

While optical methods have been extensively explored for the synthesis of thin films and bonded electrical wires (refs. 1 to 4), their utility for forming particles suitable for CNT catalysis have yet to be thoroughly tested. Therein the objective of our work was to form an incomplete thin film of catalyst particles using four optically based methods: (1) pulsed laser transfer (PLT), (2) photolytic deposition (PLD), (3) photothermal deposition (PTD) and (4) laser ablation deposition (LABD). The catalytic activity of the particles created by each of the techniques was assessed by the following criteria. The surface density of the CNT's they formed provided a gauge of the catalyst particle dispersal while the CNT diameter distribution revealed the degree of their size uniformity. Finally the structure of the catalyst particle was inferred from the extent of graphitic structures observed in the CNT's produced. The overall morphology and size of the CNT's was determined using SEM while TEM revealed the extent of graphitization in their structure. The following section describes the experimental approach, results and analysis for each method.

Technique Descriptions, Results, and Discussion

1. Pulsed Laser Transfer (PLT)

A.—Experimental Description

The pulsed laser transfer technique we used to prepare a supported catalyst for subsequent CNT synthesis is related to the technique of laser-induced forward transfer (LIFT) used in thin-film deposition. LIFT employs pulsed laser light to remove material, previously coated as a thin film on a transparent support, from that support (refs. 10 to 17). The ablation event transfers the film onto another substrate in close proximity to the film when the thin film material reaches its boiling temperature. Within the laser-irradiated region, material is propelled toward the target by the laser-generated plasma, which is trapped, between the source film and its support. As expected, higher powers and thinner films lead to better, more uniform deposition. This reflects the more uniform vapor pressure that is attained under such conditions, which thereby minimize the transfer of spall, blown-off droplets or other semi-molten fragments.

If the film is comparable to or thicker than the thermal diffusion length on the timescale of the laser pulse, the melt zone only partially penetrates the foil (ref. 18). Hence the remaining solid portion of the film serves as the support against which the explosive vaporization occurs. In this case material is then ejected back towards the laser source direction. The optically transparent substrate in front of the film then becomes the target surface. In the event that the patterned "thick" film is in direct contact with the optical window, material will force the ablated material sideways into the gaps between the film pattern. By virtue of its close proximity, the rear surface will also receive a deposited coating originating from the sideways-directed material.

Our adaptation of this technique to prepare catalysts for CNT synthesis uses a stainless steel TEM grid as the metal target, which has a type 304 (200×200) woven wire mesh. This mesh was sandwiched between two quartz plates in ambient air and subjected to a single laser pulse. Since the irradiation was performed within 1 meter of the laser exit, the pulse maintained its near-field profile and no beam conditioning was required. The 10 ns pulse at 1064 nm produced by a Nd:YAG laser had a beam diameter of 0.5 cm, which provided a laser fluence of 0.92 J cm^{-2} when operating at 180 mJ per pulse.

B.—Results and Discussion

Figure 1 shows a series of SEM images at different magnifications for the supported catalyst after being subjected to what we will refer to as our standard hydrocarbon growth run. This consisted of a 25-minute exposure at 800 °C to a C_2H_2, H_2 and He mixture at flow rates of 10, 25 and 500 sccm, respectively. The flow of this gas mixture at 1 atm also included approximately 75 Torr of benzene vapor. The lower magnification image (fig. 1(a)) illustrates the overall pattern left by the TEM grid. Figure 1(c) shows that each square consists of a dense array of CNT's, the synthesis of which was catalyzed by metal blown into the openings from the surrounding mesh wires during the laser pulse. Because the mesh wire thickness (40 um) is much larger than the thermal diffusion length of the stainless steel wire, LIFT proper of the mesh wire to the substrate did not occur. Instead, ablated material traveled back along the beam propagation direction and sideways into the open areas of the mesh. Since the TEM grid possesses a weave, the mesh wires periodically contact the backing quartz substrate. Locations where the mesh wire lifts up from the substrate create an underpass along which ablated material from the mesh can propagate. This indirect path accounts for the lower density and smaller diameters of CNT's observed in these partially shielded regions where only smaller metal particles could drift. In contrast, more vaporized material can collect with the open squares from the surrounding wires, thereby creating a higher catalyst particle density. Given the likely occurrence of sintering and coalescence processes, catalyst particles will be larger in the open areas than within the shadowed region as manifested by the different CNT diameters observed in the two regions.

The density of CNTs was highly dependent upon the incident laser pulse energy used to create the supported catalyst. For fluences below 90 mJ/cm^2, little CNT growth was observed, consistent with no transfer of metal catalyst from the mesh to either substrate (front or back). Higher fluences, such as 200 mJ/cm^2, led to CNT growth along the outline imposed by the mesh wires, consistent with their formation via the LIFT mechanism described earlier. For laser fluences beyond 300 mJ/cm^2, the mesh was visibly altered and much larger diameter CNT's and nanofibers were formed. These results can be further understood by considering the energy required to ablate the material in the process. With the thermal diffusion length of the mesh wire large relative to the wire physical diameter, uniform heating does not occur for the laser fluences and pulse durations used here [3]. Only backwards (and potentially sideways directed) LIFT can occur at the fluences used here. This then accounts for the shadowing effect imposed by the mesh wires, which would not occur if LIFT proper took place. However increasing laser fluence will heat more material to its vaporization temperature and thus generate more vapor and corresponding condensation products.

Figure 2 shows a HRTEM image of a representative CNT, which was collected by dispersing the CNT's grown on the supported catalyst onto a lacey carbon TEM grid. A multi-walled structure is evident possessing extended graphitic order and a uniform central channel. Though variations in CNT surface number density and length were observed as illustrated by the SEM images, the structure shown in figure 2 is representative of those obtained from Fe using different catalyst preparation methods.

2. Photolytic Deposition (PLD)

A.—Experimental Description

The photolytic decomposition method of catalyst preparation begins with the photodissociation of a gaseous catalyst precursor, typically an organometallic compound (ref. 19), in an inert environment. In general, these compounds possess dissociative excited electronic states at relatively low energies, which makes their photolysis by near-ultraviolet light sources feasible (ref. 20). Decomposition of the organometallic compound liberates metal atoms, which rapidly undergo nucleation, with condensation occurring at gas-kinetic rates. Nanoscale catalysts are produced through the sequential addition of atoms, small molecules and clusters to the growing particle. Convective flow or gravitational sedimentation directs the

deposition of these particles on a substrate. The irradiated volume, laser fluence, wavelength, precursor vapor pressure and ambient inert gas pressure can all be used to adjust the catalyst particle size.

We prepared the supported catalysts in a 2-in diameter cylindrical glass cell with a length of 31 cm. The photolysis was initiated by 266 nm light from a Nd:YAG laser, which propagated the entire length of the cell. Substrates to collect the deposited particles were placed along the bottom of the cell nearest the entrance window. A quartz boat containing a few grams of the organometallic compound, ferrocene, was placed on the bottom of the cell nearest the exit window. Nitrogen gas provided an inert environment and a pressure beyond the vapor pressure of ferrocene (174 mTorr) to facilitate condensation of the growing metal nanoparticles. A vacuum pump and capacitance manometers attached to the cell allowed adjustment and monitoring of the inert gas pressure. We found an inert pressure in the general range of 4 Torr to be optimal. A 3:1 telescope provided downcollimation of the beam to fluences necessary to produce nanoparticles. We used a fluence of about 600 mJ/cm^2 in our experiments.

We used two real time diagnostics to identify conditions that lead to the formation of nanoparticles. First, we checked for visible light emission along the laser beam track through the cell. Nanoparticles in the irradiated region would likely produce laser induced incandescence over a broad range of wavelengths, including the visible range. Second, we counterpropagated 532 nm light from a CW Nd:YAG laser through the cell in regions away from the photolysis laser beam track. Scattered light along the beam track of this second laser confirmed the presence of nanoparticles throughout the cell volume.

The onset of intense optical absorption in ferrocene begins near 4 eV (ref. 21), which corresponds to a charge transfer band. Dissociation begins at somewhat higher excitation energies. The photon energy of the 266 nm light used in these experiments, 4.66 eV, is insufficient to dissociate ferrocene. Thus, dissociation at 266 nm occurs via two-photon absorption. It is generally accepted that the products of the dissociation are the elemental metal atom and cyclopentadienyl radicals (refs. 22 and 23).

B.—Results and Discussion

A comparison of the CNT yield from catalyst nanoparticles deposited on quartz versus metal substrates (e.g., Mo) showed the quartz substrate to be essential to success of the method. For the metal substrates, deposited catalyst particles presumably fused with the underlying metal substrates or migrated and collected along grain boundaries. Figure 3 shows SEM images of CNT growth on supported catalysts prepared using irradiation times of 15 and 30 minutes. Results from a variety of irradiation times reveal that 15 minutes is optimal to generate sufficient amounts of deposited catalyst. This was surprising given the presence of a laser beam track through the cell for the entire irradiation time, which suggested much higher aerosol production rates. As figure 3(a) shows, this condition produced long CNT's that appeared to branch from clusters, likely reflecting the deposited catalyst distribution. A 30 minute irradiation time, however, yielded tightly bound aggregates of particles that were catalytically inactive toward CNT growth (fig. 3(b)).

The HRTEM images in figure 4 reveals the cause of relatively poor catalyst activity given the amount of aerosol production. As seen in the lower magnification image (fig. 4(b)), the catalyst particles, though of a desirable size, are imbedded within an amorphous carbon matrix much like raisins within bread pudding. This matrix likely originates from photolysis reactions that produce highly reactive organic radicals. These species readily react with small metal clusters and can also undergo gas-phase polymerization, the products of which can also condense on small metal clusters. The presence of organic carbon on the nanoparticles during CNT synthesis could facilitate carbide formation and hence deactivate the particle. Moreover, extraneous carbon fragments could provide sites for additional carbon deposition, thereby adding to the carbonaceous matrix surrounding the particles.

In light of these results, we subjected the deposited composites to a variety of pretreatments (e.g., oxidation, reduction) prior to the CVD synthesis process in an attempt to remove the carbon matrix and recover the metal nanoparticles. These efforts met with little success, however.

3. Photothermal Deposition (PTD)

A.—Experimental Description

The photothermal technique is similar to the photolytic method in that the catalyst precursor decomposes to liberate the metal atom that ultimately forms the catalyst particle. It differs from the photolytic method by using laser heating to decompose the organometallic compound (refs. 24 to 28). Heat can be deposited either through an absorbing substrate material or an absorber in the bath gas containing the precursor reagent. In the former case, rapid molecular decomposition occurs upon collision with the heated surface resulting in the deposition of metal atoms on the surface over the irradiated region. Control of the irradiation time and energy can be used to control the deposition density of the thin film that begins to form. If the deposit becomes too thick, discrete catalyst particles are no longer present to catalyze CNTs. Instead, a thin film forms that is far less active at catalyzing CNT formation. Given that the thermal decomposition will depend nonlinearly upon the surface temperature via an Arrhenius factor, there will be an apparent threshold in laser intensity for deposition. Therein the irradiation time and precursor vapor pressure are expected to be the primary variables.

We used the same 2-in diameter cylindrical glass cell to prepare supported catalysts with the photothermal method as we did for the photolytic method. A 1/4-inch square quartz substrate was mounted inside the cell to intercept the path of a 10.6 um unfocused laser beam from a 40 W CO_2 laser. A helium-neon laser beam counterpropagating through the cell along the same path as the CO_2 laser beam allowed for convenient positioning of the substrate before irradiation. A quartz boat containing a few grams of ferrocene was placed on the bottom of the cell near the KBr entrance window for the CO_2 laser. As with the photolytic experiments, nitrogen gas provided an inert environment and a pressure beyond the room temperature vapor pressure of ferrocene to facilitate condensation of the metal nanoparticles on the irradiated surface. Conditions that created a dull orange glow from the substrate in the 1/4 diameter area of the laser beam resulted in the deposition of material in the irradiated region. This visual cue showed that too high a pressure of the inert gas cooled the irradiated substrate, thus thwarting photothermal decomposition of ferrocene on its surface. It was also important that the laser beam irradiate only the substrate and not any portion of the metal holder used to position the substrate to prevent thermal loss from the substrate.

B.—Results and Discussion

Figure 5 shows SEM images of a supported catalyst prepared by photothermal dissocation of ferrocene on quartz, which was then subjected to our standard hydrocarbon growth run. The dense growth of CNT obtained shows that this method is well suited for catalyst synthesis. Preparation of this supported catalyst involved a 2-minute irradiation time of the substrate by the CO_2 laser. We found that irradiation times of 2 minutes or less produced the most viable catalysts for CNT growth with our power density of 4.2 W/cm^2. Times extending beyond 3 minutes led to the formation of a thin film whose activity towards CNT catalysis was markedly less.

4. Laser-Ablation Deposition (LABD)

A.—Experimental Description

The laser ablation-deposition approach uses pulsed laser light to break up a target of the desired metal. Condensation products from the ablation plume created then deposit upon a substrate placed in close proximity (refs. 29 to 34). One approach is to place the substrate to be coated directly in the path of the ablation plume. The initial kinetic energy of the plume then serves to promote adherence of the deposited material or even to implant the material into the target.

An alternative approach used here to render a more direct comparison with the photolytic decomposition technique is to allow gravitational sedimentation of the growing metal clusters from the expansion plume upon a substrate. Variations in the CNT yield, morphology and internal structure can then be used

to infer the activity of the catalyst particle, its structure and possible complications from impurities. To create the metal nanoparticles, a Nd:YAG laser ablates a rotating metal disk of iron within a stainless steel cell. The substrates to be coated are placed along the bottom of the cell approximately 2.5, 7, and 13 cm from the rotating target. A vacuum system and capacitance manometer allowed for the introduction of various gases and for adjustment of the ambient pressure. The supported catalysts obtained were then subjected to our standard hydrocarbon run.

B.—Results and Discussion

The laser energy, focussing conditions, target material density and structure, backing gas pressure and identity can all be used to control the ablation plume density and expansion and hence the resulting catalyst particle size, composition and spatial distribution upon the substrate. Among these we found the backing gas pressure, identity and deposition time to be the dominant parameters. Supported catalysts prepared in inert gases (Ar or He) or reactive gases (e.g., O_2) at atmospheric pressure gave poor CNT yields, as illustrated in figure 6(a). The aligned particle clusters shown in the figure may result from the magnetic properties of the iron nanoparticles and their aggregates. In general, these conditions produced clusters of particles for which the relative density and degree of alignment vary with pressure, laser fluence and deposition time.

As figure 6(b) illustrates, the best results were achieved by using low ambient pressures of O_2, typically 100 mTorr. Pressure in this range result in a greater degree of plume expansion, thereby slowing the rates of both particle growth and clustering. Thus, the clusters formed and the particles they contain would be smaller with a greater exposed surface area (ref. 2). Furthermore, the O_2 would react with hot metal vaporization products to form an oxide aerosol phase. The oxide particles would likely resist coalescence to a greater extent than reduced metal particles in the aerosol phase and would also resist ripening prior and subsequent to deposition. In the absence of O_2, partial sintering during condensation of the cooling metal plume could mismatch lattice planes of neighboring crystallites, rendering them inactive towards carbon solvation and dissolution, fundamental steps in CNT synthesis (refs. 35 to 38). Results from supported catalysts prepared in an H_2 ambient environment (fig. 6(c)) show aggregates of particles that appear highly sintered, somewhat similar to the photolytic results at high laser fluences. As with the PLD results under those conditions, these aggregates also proved inactive towards CNT catalysis. All of these results suggest that coalescence and ripening are responsible for deactivation of the catalyst particles produced in the inert or reducing environments. This explanation also accounts for the viability of catalysts produced in O_2 with backing pressures of up to a few Torr.

Figure 7 shows results from a supported catalyst produced at a reduced pressure (100 mTorr) in an inert gas environment (He). Though individual particles within the clusters observed are suitably sized for CNT catalysis, these particles were generally inactive for reasons that are presently unclear.

Conclusions

The work presented tests four approaches for depositing catalyst particles for CNT synthesis and compares their viability. Each method possesses potential advantages not all of which were realized under our test conditions. We found the best method tested to be PLT, followed by PTD, and then the ABD and PLD methods, which were roughly comparable.

The PLT resulted in the most dense and uniform catalyst particles and was capable of producing the finest patternation. The photothermal method produced similar results, but was dependent upon the organometallic vapor pressure and required significant processing time. Its utility could be realized in writing catalyst patterns through either beam or substrate rastering. The photolytic technique also proved to be time consuming. Inherent in the PLD process is the generation of reactive organic photoproducts that

likely react in the gas phase with hot metal clusters under the action of the pulsed laser heating. The result is metal catalyst particles imbedded within amorphous carbon. Post treatments prior to CVD such as reduction or mild oxidation did not liberate and activate the catalyst particles.

Each technique yielded a variety of CNT diameters with varying levels of extended graphitic order. In addition to CNT's, other types of nanofibers were synthesized including spirals and solid nanofibers. The relative distribution of product types, their graphitic structure and relative surface coverage were highly dependent upon the catalyst particle synthesis conditions.

References

1. Osgood, R.M.; Gilgen, H.H.: Ann. Rev. Mater. Sci. 1985, 15, 549.
2. Chrisey, D.B.; Hubler, G.K.: Pulsed Laser Deposition of Thin Films; John Wiley and Sons, Inc.; New York, 1994.
3. Bauerle, D.: Chemical Processing with Lasers; Springer-Verlag; New York, 1986.
4. Eden, J.G.: Photochemical Vapor Deposition; John Wiley and Sons, Inc.; New York,1992.
5. Kirk-Othermer Encyclopedia of Chemical Technology, 4th ed.; Wiley Interscience; New York, 1999.
6. Zhang, Z.; Lagally, M.G.: Science 1997, 276, 377.
7. Park, J-H., Ed.: Chemical Vapor Deposition, Surface Engineering Series, Vol. 2; ASM International; 2001.
8. Sinnott, S.B.; Andrews, R.; Qian, D.; Rao, A.M.; Mao, Z.; Dickey, E.C.; Derbyshire, F.: Chem. Phys. Lett. 1999, 315, 25.
9. Collins, P.G.; Avouris, P.: Scientific American 2000, 283, 38.
10. Zaleckas, V.J.: Appl. Phys. Lett. 1977, 31, 615.
11. Al-Nimr, M.A.; Masoud, S.A.: J. Heat Trans.-T ASME 1997, 119, 188.
12. Esrom, H.; Zhang, J-Y; Kogelschatz, U.; Pedraza, A.J.: Appl. Surf. Sci. 1995, 86, 202.
13. Pimenov, S.M.; Shafeev, G.A.; Smolin, A.A.; Konov, I.V.; Vodolaga, B.K.: Appl. Surf. Sci. 1995, 86, 208.
14. Tóth, Z.; Solis, J.; Afonso, C.N.; Vega, F.; Szörényi, T.: Appl. Surf. Sci. 1993, 69, 330.
15. Bohandy, J.; Kim, B.F.; Adrian, F.J.: J. Appl. Phys. 1986, 60, 1538.
16. Kántor, Z.; Tóth, Z.; Szörényi, T.: Appl. Phys. 1992, 54, 170.
17. Montgomery, R.K.; Mantei, T.D.: Appl. Phys. Lett. 1986, 48, 493.
18. Adrian, F.J.; Bohandy, J.; Kim, B.F.; Jette, A.N.; Thompson, P.J.: Vac. Sci. Technol. B 1987, 5, 1490.
19. Buono-Core, G.E.; Tejos, M.; Lara, J.; Aros, F.; Hill, R. H.: Mat. Res. Bull. 2000, 34, 2333.
20. Bottka, N.; Walsh, P.J.; Dalbey, R.Z.: J. Appl. Phys. 1983, 54, 1104.
21. Stauf, G.T.; Driscoll, D.C.; Dowben, P.A.; Barfuss, S.; Grade, M.: Thin Solid Films 1987, 153, 421.
22. Leutwyler, S.; Even, U.; Jortner, J.: Chem. Phys. Lett. 1980, 74, 11.
23. Liou, H.T.; Ono, Y.; Engelking, P.C.; Moseley, J.T.: J. Phys. Chem. 1986, 90, 2888.
24. Fitz-Gerald, J.M.; Piqué, A.; Chrisey, D.B.; Rack, P.D.; Zeleznik, M.; Auyeung, R. C. Y.; Lakeou, L.: Appl. Phys. Lett. 2000, 76, 1386.
25. Fisanick, G.J.; Hopkins, J.B.; Gross, M.E.; Fennell, M.D.; Schnoes, K.: J. Appl. Phys. Lett. 1985, 46, 1184.
26. Gupta, A.; Jagannathan, R.: Appl. Phys. Lett. 1987, 51, 2254.
27. Gross, M.E.; Fisanick, G.J.; Gallagher, P.K.; Schnoes, K.J.; Fennell, M.D.: Appl. Phys. Lett. 1985, 47, 923.
28. Allen, S.D.; Jan, R.Y.; Mazuk, S.M.; Vernon, S.D.: J. Appl. Phys. 1985, 58, 327.
29. Timm, R.; Willmott, P.R.; Huber, J.R.: J. Appl. Phys. 1996, 80, 1794.

30. Misra, A.; Thareja, R. K.: J. Appl. Phys. 1999, 86, 3438.
31. Wang, H.; Salzberg, A.P.; Weiner, B.R.: Appl. Phys. Lett. 1991, 59, 935.
32. Misra, A.; Mitra, A.; Thareja, R.K.: Appl. Phys. Lett. 1998, 74, 929.
33. Tambay, R.; Singh, R.; Thareja, R.K.: J. Appl. Phys. 1992, 72, 1197.
34. Abhilasha, P.; Prasad, S.R.; Thareja, R.K.: Phys. Rev. E. 1993, 48, 2929.
35. Rodriguez, N.M.: J. Mater. Res. 1993, 8, 3233.
36. Baker, R.T.K.; Harris, P.S.; Thomas, R.B.; Waite, R.J.: J. Catal. 1973, 30, 86.
37. Tibbets, G.G.; Devour, M.G.; and Rodda, E.J.: Carbon 1987, 25, 367.
38. McAllister, P.; Wolf, E.E.: J. of Catal. 1992, 138, 129.

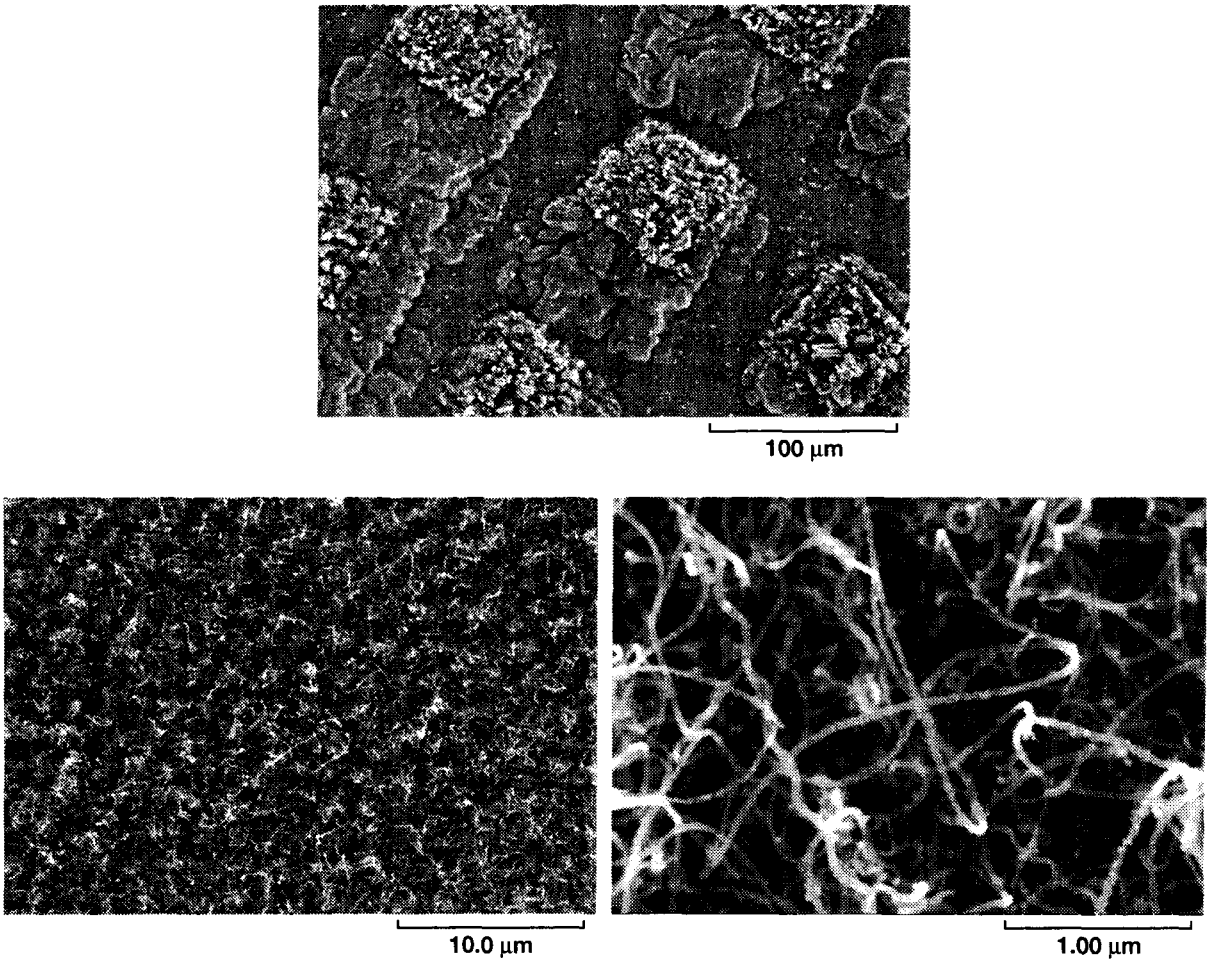

Figure 1.—Pulsed laser transfer catalyst preparation using a SS TEM grid as template.

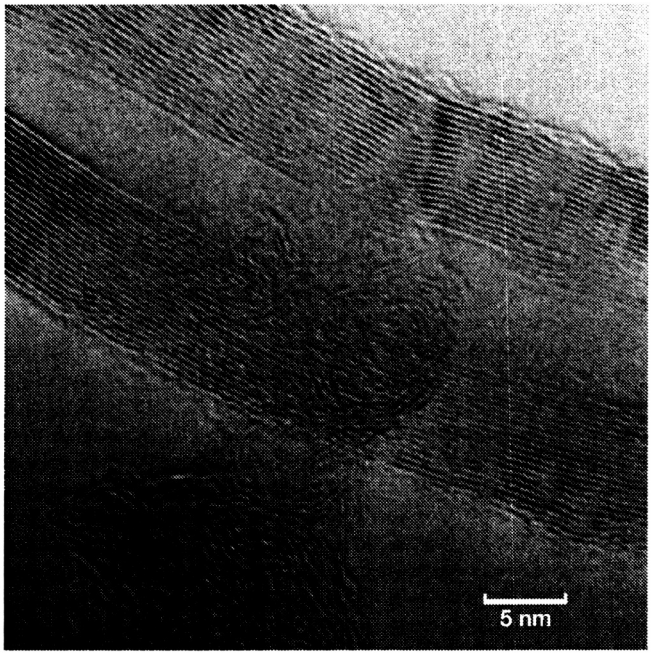

Figure 2.—HRTEM image of catalytic material from the PLT process.

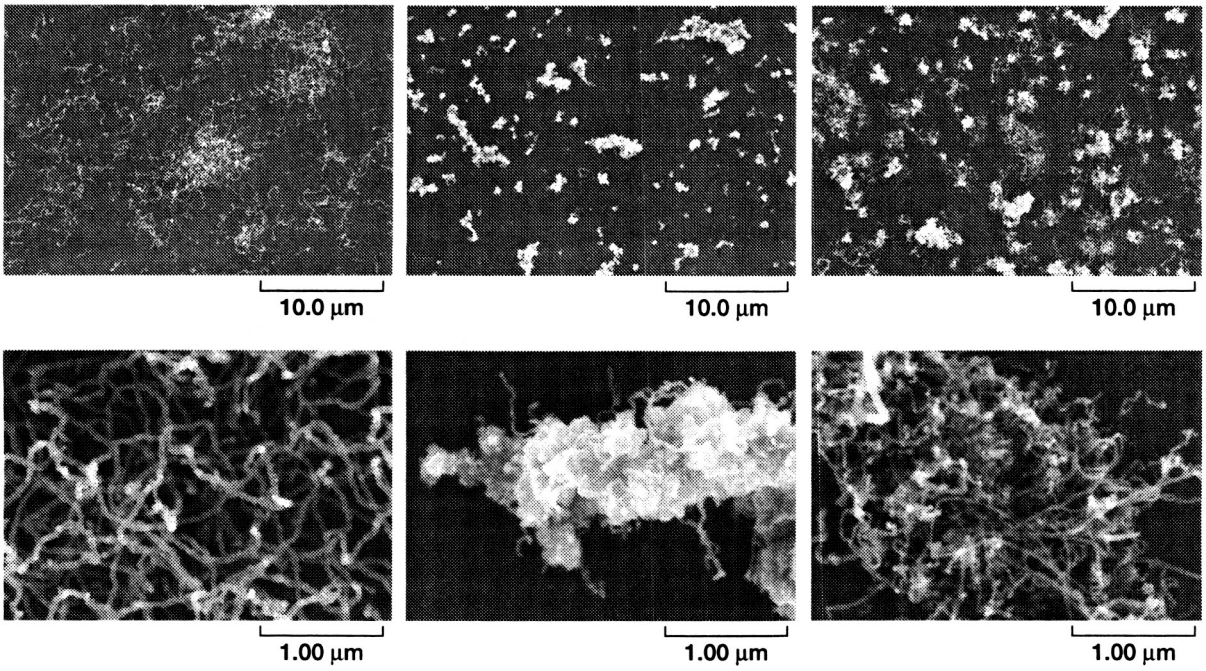

Figure 3.—Photolytic catalyst preparation using $FeCp_2$.

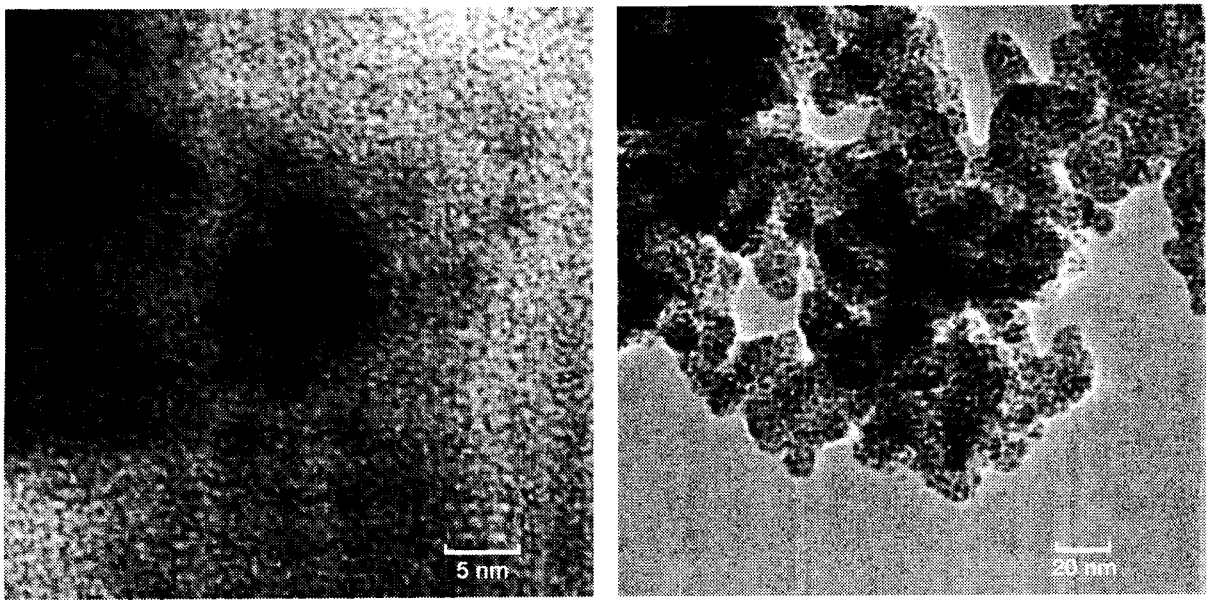

Figure 4.—HRTEM images of catalytic material from the PLT process.

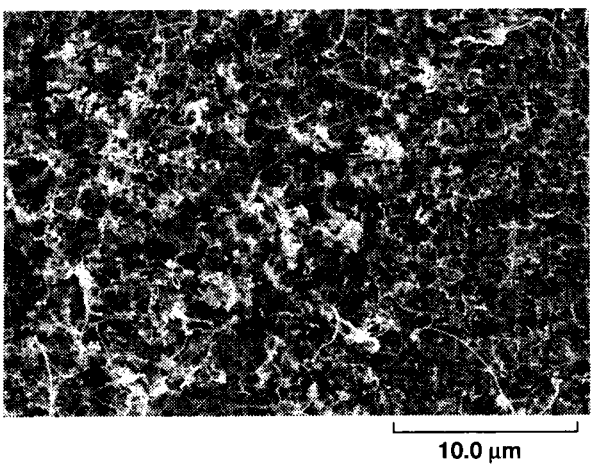

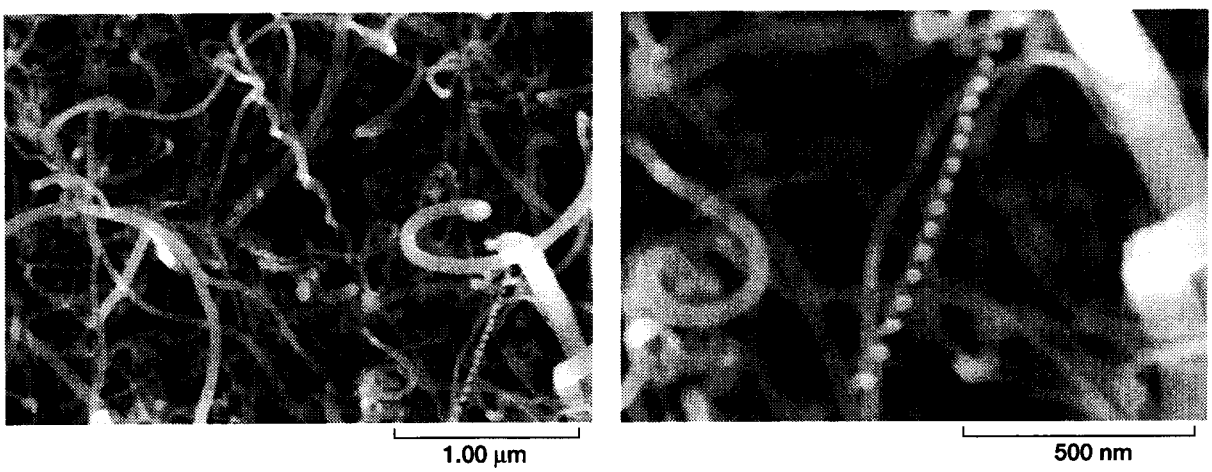

Figure 5.—Photolytic catalyst preparation using $FeCp_2$.

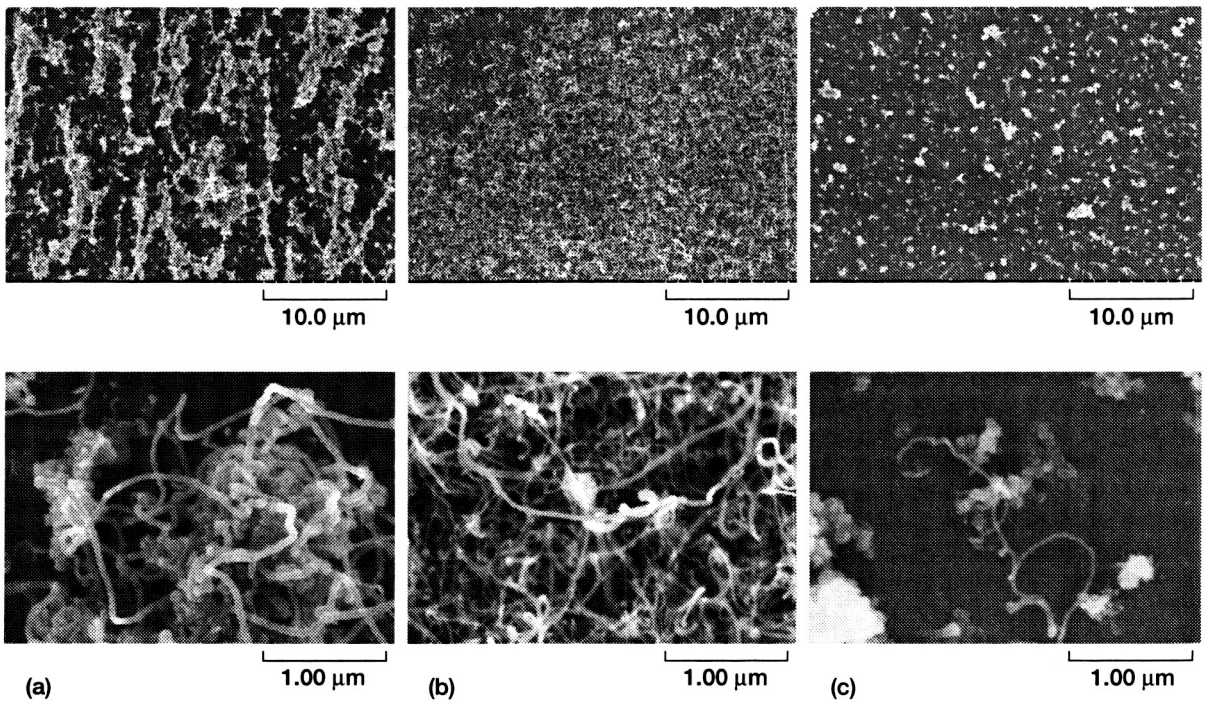

Figure 6.—Pulsed laser ablation catalyst preparation using Fe target. (a) He 1 atm. (b) O_2 150 mTorr. (c) H_2 1 atm.

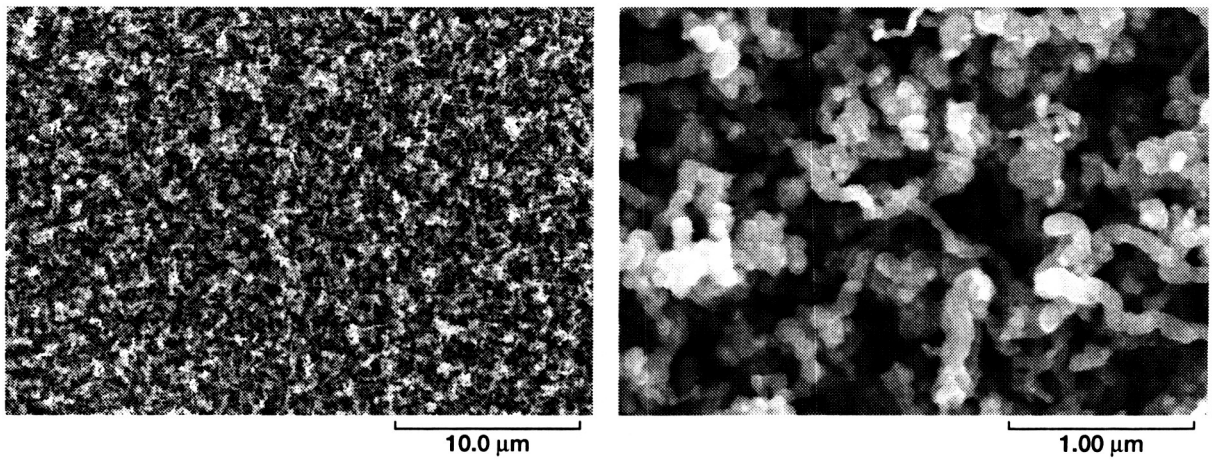

Figure 7.—Pulsed laser ablation catalyst preparation using Fe target in He at 150 mTorr.

REPORT DOCUMENTATION PAGE

Form Approved
OMB No. 0704-0188

1. AGENCY USE ONLY (*Leave blank*)	2. REPORT DATE	3. REPORT TYPE AND DATES COVERED
	September 2003	Final Contractor Report

4. TITLE AND SUBTITLE

Laser Synthesis of Supported Catalysts for Carbon Nanotubes

5. FUNDING NUMBERS

WBS–22–101–12–06
NCC3–975

6. AUTHOR(S)

Randall L. Vander Wal, Thomas M. Ticich, Leif J. Sherry, and Lee J. Hall

7. PERFORMING ORGANIZATION NAME(S) AND ADDRESS(ES)

National Center for Microgravity Research
21000 Brookpark Road
Cleveland, Ohio 44135

8. PERFORMING ORGANIZATION REPORT NUMBER

E–14122

9. SPONSORING/MONITORING AGENCY NAME(S) AND ADDRESS(ES)

National Aeronautics and Space Administration
Washington, DC 20546–0001

10. SPONSORING/MONITORING AGENCY REPORT NUMBER

NASA CR—2003-212582

11. SUPPLEMENTARY NOTES

Randall L. Vander Wal and Lee J. Hall, National Center for Microgravity Research, Cleveland, Ohio 44135; Thomas M. Ticich and Leif J. Sherry, Centenary College of Louisiana, Department of Chemistry, 2911 Centenary Blvd., Shreveport, Louisiana 71134. Project Manager, Kathy Schubert, Microgravity Science Division, NASA Glenn Research Center, organization code 6700, 216–433–5331.

12a. DISTRIBUTION/AVAILABILITY STATEMENT

Unclassified - Unlimited
Subject Category: 99 Distribution: Nonstandard

Available electronically at http://gltrs.grc.nasa.gov

This publication is available from the NASA Center for AeroSpace Information, 301–621–0390.

12b. DISTRIBUTION CODE

13. ABSTRACT ***(Maximum 200 words)***

Four methods of laser assisted catalyst generation for carbon nanotube (CNT) synthesis have been tested. These include pulsed laser transfer (PLT), photolytic deposition (PLD), photothermal deposition (PTD) and laser ablation deposition (LABD). Results from each method are compared based on CNT yield, morphology, and structure. Under the conditions tested, the PLT was the easiest method to implement, required the least time, and also yielded the best patternation. The photolytic and photothermal methods required organometallics, extended processing time and partial vacuums. The latter two requirements also held for the ablation deposition approach. In addition to control of the substrate position, controlled deposition duration was necessary to achieve an active catalyst layer. Although all methods were tested on both metal and quartz substrates, only the quartz substrates proved to be inactive towards the deposited catalyst particles.

14. SUBJECT TERMS

Carbon nanotube synthesis; Laser catalyst synthesis; Supported catalyst synthesis

15. NUMBER OF PAGES
17

16. PRICE CODE

17. SECURITY CLASSIFICATION OF REPORT	18. SECURITY CLASSIFICATION OF THIS PAGE	19. SECURITY CLASSIFICATION OF ABSTRACT	20. LIMITATION OF ABSTRACT
Unclassified	Unclassified	Unclassified	